Available online at www.sciencedirect.com

ScienceDirect

Procedia CIRP 111 (2022) 588–591

www.elsevier.com/locate/procedia

12th CIRP Conference on Photonic Technologies [LANE 2022], 4-8 September 2022, Fürth, Germany

Thermal signature of LIPSS formation revealed by infrared diagnostics

Jiří Martan[a,*], Carlos Beltrami[a], Petr Hauschwitz[b], Denys Moskal[a], Radka Bičišťová[b], Milan Honner[a], Alexander Brodsky[c], Vladislav Lang[a]

[a]*New Technologies Research Centre (NTC), University of West Bohemia, Univerzitni 8, 30100 Plzen, Czech Republic*
[b]*Hilase Centre, Institute of Physics, Academy of Sciences of the Czech Republic, Za Radnici 828, Dolni Brezany 25241, Czech Republic*
[c]*R&D Department, Holo/Or Ltd, Einstein 13b, Ness Tziona 7403617, Israel*

* Corresponding author. Tel.: +420-37763-4718; *E-mail address:* jmartan@ntc.zcu.cz

Abstract

Formation of Laser Induced Periodic Surface Structures (LIPSS) is a very interesting phenomenon. As the process is now moving towards the industry for the production of functional surfaces, a monitoring technique for online process control is needed. In the present work, the process was investigated for the first time using fast infrared radiometry. An advanced multi-beam laser system with 2601 beams using DOE and 200 W picosecond laser was used. Heat accumulation was measured during the 50 pulses of LIPSS fabrication on steel for fluences from 0.07 to 0.31 J/cm^2 and frequency 50 kHz. Interestingly, on the cooling part of the curves, plateaus were observed after each laser pulse, for high pulse energies even double plateaus. The observed shapes of the signal evolution in time represent thermal signature of the LIPSS formation. The results are promising that process control will be feasible by monitoring heat accumulation or plateau length.

Keywords: laser surface nanostructuring; temperature measurement; heat accumulation; process monitoring and control; multibeam

1. Introduction

Laser Induced Periodic Surface Structures (LIPSS) are organized nanostructures or microstructures induced by ultrashort laser pulses on the surface of the material. They are an arrangement of (quasi)periodic topographic lines representing a linear surface grating structure. They have gained significant attention due to the simplicity and robustness of the single process step required for their manufacturing that can be performed in ambient air [1].

In general, laser micromachining or surface texturing is still limited by low processing speed. When increasing processing speed, laser process include high power lasers and high pulse energies, which can lead to unwanted thermal degradation [2,3]. LIPSS seems to be promising in this point of view [4].

However, the thermal processes during LIPSS creation were rarely observed in-situ. It was observed by pump-probe reflectivity imaging in [5]. Thermal processes and surface temperature in ultrashort pulsed laser ablation are usually studied by numerical modelling and microscopy of the final resulting structure [3,6]. Time resolved measurements of laser heating, melting, vaporization and oxidation were done for laser pulse durations from milliseconds to nanoseconds by measuring reflectivity, transmissivity, emission and electrical conductance [7,8]. But for ultrashort pulsed laser ablation, only recently an infrared radiometry measurement system was developed and applied for ultrashort pulse laser micromachining [9].

In the present work, thermal processes during LIPSS formation were measured in-situ by infrared radiometry for the first time. The aim was to experimentally observe their dynamics and to confirm if there are phase changes involving latent heat happening during the LIPSS formation. The observed shapes of the signal evolution in time represent a thermal signature of the LIPSS formation.

10.1016/j.procir.2022.08.156

2. Experimental

For the experiment, a 200 W average power solid-state ultrashort pulsed picosecond laser (Perla C, Hilase) was used. It had a pulse duration of 1.2 ps, wavelength of 1030 nm, repetition frequency of 50 kHz and nearly Gausian distribution with M^2<1.2. The laser beam was divided into 51 x 51 (2601) beams by diffractive optical element (DOE, Holo/Or). Each spot size was about 15 µm in diameter and placed with a period of about 20 µm. The total size of one multi-beam laser spot was about 1 mm. The laser beam was positioned by a galvo scanner (Scanlab, IntelliScan 14). A detailed description of the setup can be found in [10]. The sample material was stainless steel AISI 304, with surface roughness R_a=0.1 µm.

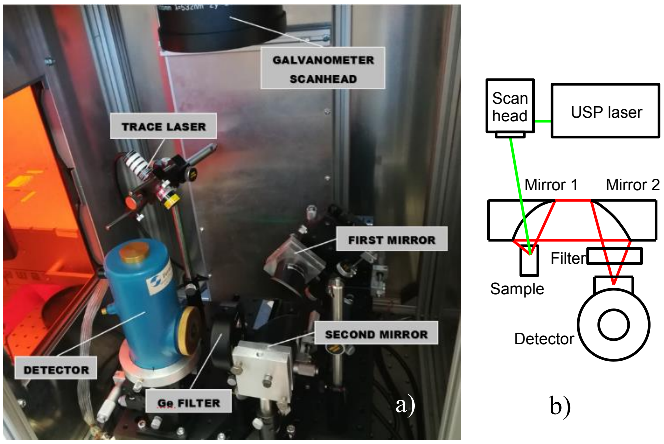

Fig. 1. The configuration of the measuring system: a) photo, b) schema.

The measuring system of fast infrared radiometry was developed in the previous work [9]. It was used for heat accumulation measurement in laser micromachining. In the present work, the investigation was widened to more thermal processes. The measuring system consisted of fast infrared (IR) detector HgCdTe (Fermionics PV-11-1) cooled by liquid nitrogen, two parabolic mirrors and an antireflection coated germanium filter. The wavelength range of the detector was from 1.5 to 12 µm. Its response time was 60 ns. The effective focal lengths (EFL) of the mirrors were: first mirror EFL = 38.1 mm, second mirror EFL = 101.6 mm, and diameter was about 50 mm. The photo of the measuring system is shown in Fig. 1. The infrared radiation from the sample went to the first mirror, to the second mirror and through the germanium filter to the detector. The detector was connected to an oscilloscope. The oscilloscope registered the voltage signal. Then the detector needs to be calibrated to specific optical and laser configuration to obtain temperatures.

Table 1. Laser parameters in the LIPSS processing. Frequency was 50 kHz.

Average power (W)	Pulse energy (mJ)	Average fluence (J/cm^2)
30	0.6	0.07
50	1.0	0.12
70	1.4	0.17
100	2.0	0.24
130	2.6	0.31

The parameters of the laser process are shown in Tab. 1.. The multibeam laser spot was steady on one place of the sample for the defined number of laser pulses from 1 to 50. During this process, thermal radiation in IR wavelengths was measured. Then, for the next process, the sample was moved. Therefore, each process took place in an unprocessed area. Heat accumulation (HA) signal was measured as a signal just before the next laser pulse. Plateau length was determined by a signal derivation approach [10].

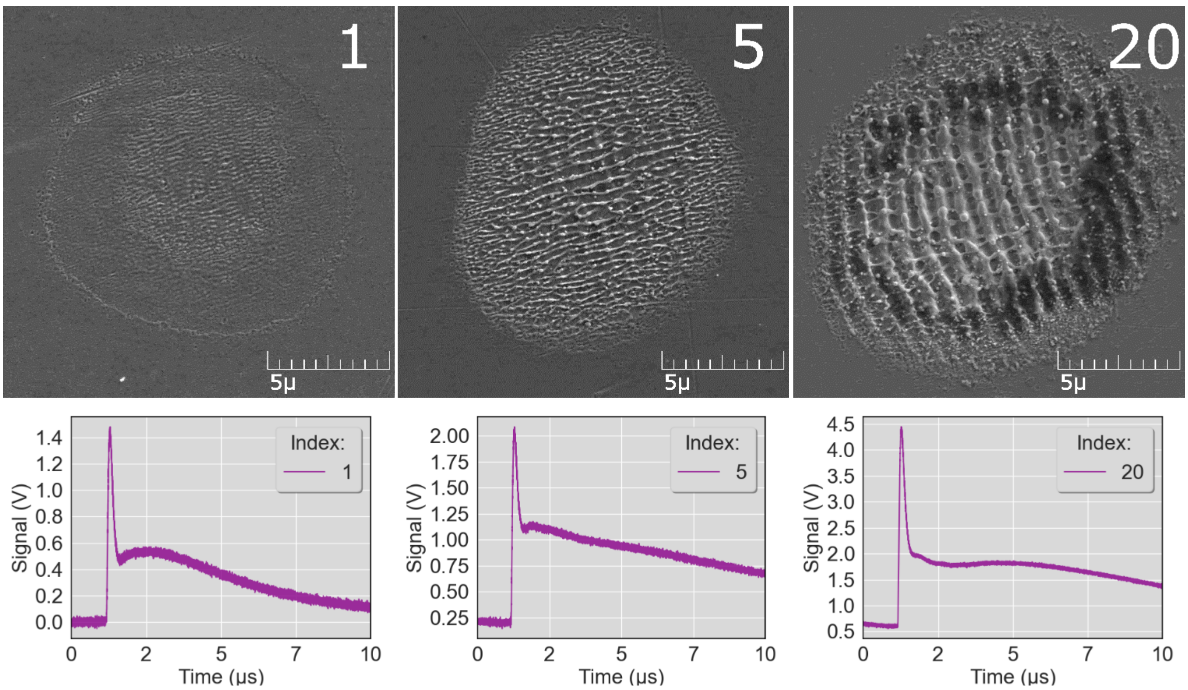

Fig. 2. SEM images of nano- and microstructures (LIPSS) produced with fluence 0.31 J/cm^2 and different number of pulses (1, 5, 20) and corresponding measured IR radiation curves.

3. Results and discussion

Examples of the produced surface structures and corresponding IR radiometry results are shown in Fig. 2. SEM micrographs show subtle ablation of the surface (1st pulse), High Spatial Frequency LIPSS (HSFL, 5th pulse) and Low Spatial Frequency LIPSS (LSFL, 20th pulse).

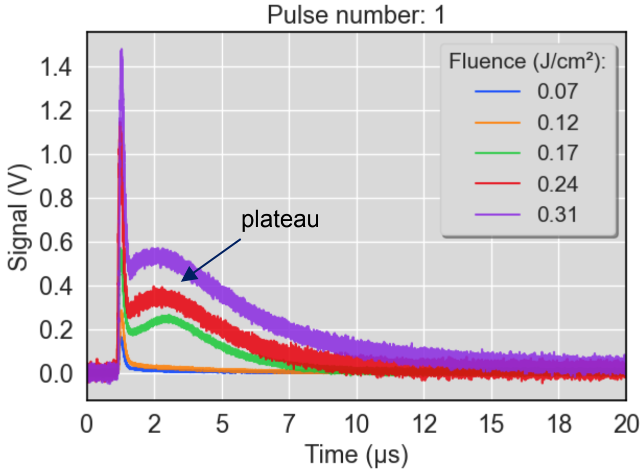

Fig. 3. IR radiometry signal evolution in time for the first laser pulse and different fluences.

Fig. 3 shows IR radiometry signal after the first laser pulse. The signal contains a sharp peak and then, in most cases, an abrupt change in the trend of the signal during the cooling phase. This change, called a plateau, is either in form of a constant signal for a certain time or a wide convex curve with a local maximum. In the case where there would be only heating and cooling, the cooling curve would be continuously exponentially decreasing (as it is almost in the case of fluences 0.07 and 0.12 J/cm^2). The plateau can be explained by a phase change (e.g. solidification) [8]. In some cases, there is first an undercooling and then the convex shape of the curve for a certain time in the plateau. The sharp peak at the beginning, just after the laser pulse, is mainly caused by thermal radiation of the overheated liquid phase and emission of radiation from plasma induced by the laser pulse over the surface.

The convex shape plateaus appear for higher fluences for the first laser pulse. The height of the top level of the plateau is increasing with the increase of fluence. The plateau length stays constant. The different height of the plateau is strange for the case of melting. A constant value would be expected due to the constant temperature value of the solidification phase change. The increasing value can be caused by the increasing size of the melted area on the surface, which is also observed on the SEM images.

On the other hand, the plateau was not expected to be induced by an ultrashort laser pulse. It was measured for nanosecond laser [8], but for picosecond laser, melting was not expected. Here the plateau appearing correlates with LIPSS formation on the surface. This indicates that LIPSS formation involves a phase change with a latent heat.

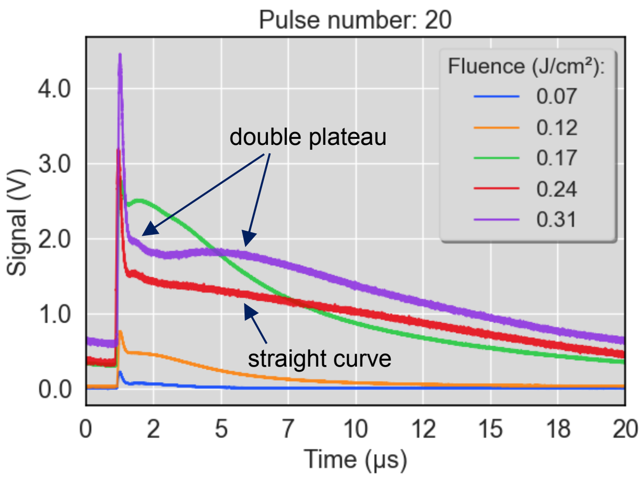

Fig. 4. IR radiometry signal evolution in time for the 20th laser pulse and different fluences.

With the repetition of laser pulses on the surface the shape of the measured signal changes to form even more complex forms. Results for 20 pulses on one place are shown in Fig. 4. For the fluence 0.12 J/cm^2, the plateau shape is flat. For the highest fluences, there is a short plateau just after the fast signal decrease and later a long plateau. This complex shape composed of two plateaus (double plateau) seems like the convolution of two curves together. Like a mixture of signals from two different processes. In the intermediate region (high number of pulses of middle fluence or lower number of pulses of high fluence), the two signals are close to each other and producing a longer plateau with two bumps or a very straight decreasing curve (not exponentially).

On the graph of IR radiometry signal with repeated pulses (Fig. 4), there can be seen an increased signal level before the laser pulse. It is caused by residual heat from previous laser pulses manifesting as increased surface temperature and is called a heat accumulation (HA) signal. The HA signal is significant mainly for the high fluence laser pulses.

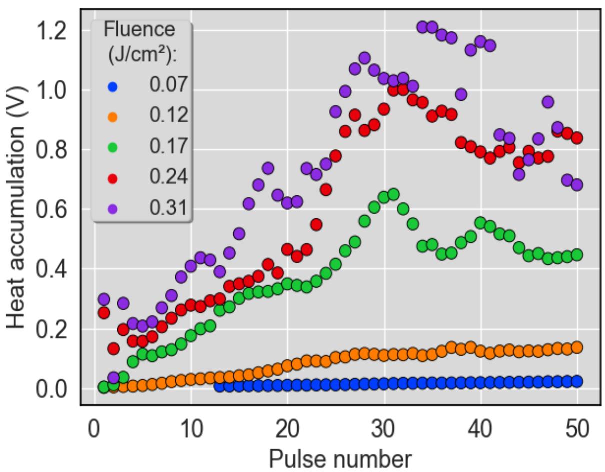

Fig. 5. Heat accumulation evolution with a number of pulses for different fluences.

The heat accumulation (HA) signal evolution with increasing number of pulses is shown in Fig. 5. It has a different shape for different fluences. For low fluences (0.07 and 0.12 J/cm^2), there is a slow continuous increase of heat accumulation signal with a number of pulses. After 30 pulses, the increase is slightly reduced for 0.12 J/cm^2. For higher fluences (0.17 to 0.31 J/cm^2), there is a strong or step increase of heat accumulation signal after the first pulse or few laser pulses. Then there is a short stable value of HA, and after that it continuously grows with some instabilities up to the maximum at 30 to 35 laser pulses, and then HA moderately decreases until the end of sequence at 50 pulses. The value of HA signal at slope change for the fluence 0.12 J/cm^2 at 30 pulses (0.1 V) is corresponding to the value step change for 0.17 J/cm^2 at 4th to 7th pulse (0.11 V) and for 0.24 J/cm^2 at 2nd to 5th pulse (0.16 V). The values for 0.31 J/cm^2 are highly oscillating around a slightly higher value of HA (0.21 V).

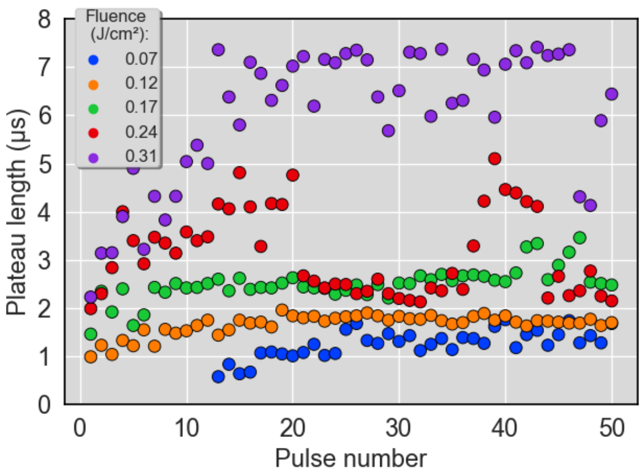

Fig. 6. Plateau length evolution with a number of pulses for different fluences.

The plateau length evolution with increasing number of pulses is shown in Fig. 6. For low number of pulses, the plateau length increases continuously with the number of pulses. The different duration of the phase change (plateau) can be easily explained by different amount of liquid phase (thickness of melt). After 15 laser pulses, the plateau length remains almost constant, but different for each fluence value. One exception is the fluence of 0.24 J/cm^2, where the determination algorithm is unstable due to the strange shape of the measured curves (almost straight decrease of the signal with time).

Concerning process monitoring and control, when the HA signal overpasses some threshold, LIPSS formation can be confirmed, e.g. 0.3 V for high fluences. And if it rises too much, global melting and surface damage (black areas) appear, e.g. 0.5 V for high fluences. The plateau length can be used either to check the laser fluence, by using the stabilized value of the plateau length, or to verify the stability of the produced structures, by observing at what number of pulses the stable value is attained. These values are probably material dependent and will have to be evaluated for each processed material.

4. Conclusion

In the present work, time resolved IR radiometry signal curves obtained during LIPSS formation were shown and analyzed. The curves represent the ongoing thermal processes on the surface of the material and their dynamics. Phase change plateaus were found in the cooling part of the signals, when HSFL LIPSS formation was observed on the surface. Double plateaus were observed when the intensive surface change was done combining LSFL LIPSS with significant amount of melt and damaged black surface areas. The IR radiometry results confirmed an important hypothesis, that LIPSS formation involves a phase change process (e.g. melting and solidification). The observed curves shapes represent the thermal signature of the LIPSS formation by ultrashort laser pulses.

Acknowledgements

The work has been supported by the Technology Agency of the Czech Republic (M-era.Net project ADVENTURE, No. TH75020001), the Ministry of Education, Youth and Sports of the Czech Republic (OP RDE program, LABIR-PAV project, No. CZ.02.1.01/0.0/0.0/18_069/0010018) and SGS-2022-007 project. The work has been also supported by Holo/Or LTD.

References

[1] Bonse J. Quo vadis LIPSS?—recent and future trends on laser-induced periodic surface structures. Nanomaterials 2020;10:1–19. https://doi.org/10.3390/nano10101950.

[2] Martan J, Moskal D, Kučera M. Laser surface texturing with shifted method — Functional surfaces at high speed. J Laser Appl 2019;022507:1–9. https://doi.org/10.2351/1.5096082.

[3] Neuenschwander B, Jaeggi B, Zimmermannn M, Markovic V, Resan B, Weingarten K, et al. Laser surface structuring with 100 W of average power and sub-ps pulses. J Laser Appl 2016;28:022506. https://doi.org/10.2351/1.4944104.

[4] Mezera M, Römer GRBE. Model based optimization of process parameters to produce large homogeneous areas of laser-induced periodic surface structures. Opt Express 2019;27:6012. https://doi.org/10.1364/oe.27.006012.

[5] Garcia-Lechuga M, Puerto D, Fuentes-Edfuf Y, Solis J, Siegel J. Ultrafast Moving-Spot Microscopy: Birth and Growth of Laser-Induced Periodic Surface Structures. ACS Photonics 2016;3:1961–7. https://doi.org/10.1021/acsphotonics.6b00514.

[6] Faas S, Bielke U, Weber R, Graf T. Prediction of the surface structures resulting from heat accumulation during processing with picosecond laser pulses at the average power of 420 W. Appl Phys A Mater Sci Process 2018;124:1–9. https://doi.org/10.1007/s00339-018-2040-4.

[7] Hatano M, Moon S, Lee M, Grigoropoulos CP, Suzuki K. Excimer laser-induced melting and resolidification dynamics of silicon thin films. JKorean PhysSoc 2001;39:S419--S424.

[8] Martan J, Cibulka O, Semmar N. Nanosecond pulse laser melting investigation by IR radiometry and reflection-based methods. Appl Surf Sci 2006;253:1170–7. https://doi.org/10.1016/j.apsusc.2006.01.077.

[9] Martan J, Prokešová L, Moskal D, Ferreira de Faria BC, Honner M, Lang V. Heat accumulation temperature measurement in ultrashort pulse laser micromachining. Int J Heat Mass Transf 2021;168:120866. https://doi.org/10.1016/j.ijheatmasstransfer.2020.120866.

[10] Hauschwitz P, Martan J, Bičišťová R, Beltrami C, Moskal D, Brodsky A, et al. LIPSS-based functional surfaces produced by multi-beam nanostructuring with 2601 beams and real-time thermal processes measurement. Sci Rep 2021;11:1–10. https://doi.org/10.1038/s41598-021-02290-3.